IEEE Access
Multidisciplinary ⋮ Rapid Review ⋮ Open Access Journal

Received 12 July 2024, accepted 26 August 2024, date of publication 2 September 2024, date of current version 10 September 2024.

Digital Object Identifier 10.1109/ACCESS.2024.3452974

RESEARCH ARTICLE

A Microstrip Antenna Achieves Dual Polarization Conversion by Rotating Metasurface

BO WU[1], PENGDONG JI[1,2], YANG LI[2], ZHENWEI LIU[2], LIANG ZHANG[2], ZHONGXIANG ZHANG[2], AND MENG KONG[2]

[1]School of Electronics and Information Engineering, Anhui University, Hefei 230039, China
[2]Anhui Province Key Laboratory of Simulation and Design for Electronic Information System, Hefei Normal University, Hefei 230601, China

Corresponding author: Meng Kong (kongmeng-2006@163.com)

This work was supported in part by Anhui Science and Technology Project 202104a05020004, and in part by the Key Project of Natural Science Research of University of Anhui Province of China under Grant 2022AH040290 and Grant KJ2021A0908.

ABSTRACT To expand the channel capacity of a traditional single-polarization reconfigurable antenna, a design method for a dual-polarization reconfigurable microstrip antenna loaded with a passive metasurface was proposed. By utilizing the equivalent circuit method and characteristic modeling analysis, this method can provide guidance for designing an integrated antenna with adjustable dual-polarization. An antenna with an operating frequency of 3.5 GHz is designed, which is composed of four layers, from top to bottom: metasurface layer, radiation patch layer, feed layer, and reflector layer. By rotating the metasurface layer to adjust its relative position with other fixed layers, the designed antenna can achieve a mutual transformation between orthogonal dual-linear polarization (Horizontal polarization/Vertical polarization) and orthogonal dual-circular polarization (Left-handed circular polarization/Right-handed circular polarization), while ensuring antenna performance. The simulation and measurement results of the designed antenna demonstrate that it possesses competitive gain and polarization isolation performance, with a 3 dB axial ratio bandwidth reaching 17.4% in the dual-circular polarization state.

INDEX TERMS Dual-polarization, metasurface, microstrip antenna, polarization reconfiguration.

I. INTRODUCTION

To meet the requirements of contemporary wireless communication systems, antennas have evolved towards integration [1], [2], broadband and multipolarization support [3], [4], and low power consumption [5]. Recently, metasurfaces (MS) have been applied in the field of antennas to flexibly adjust the characteristics of radiated electromagnetic waves [6], [7], [8], resulting in what are known as reconfigurable MS antennas [9], [10], [11].

Reconfigurable MS antennas can be classified into active and passive types. When loading an active MS, the working mode of the MS antenna is reconstructed by connecting an external programmable active device, allowing for flexible control over the electromagnetic wave characteristics [12], [13]. Active MS has also been creatively developed as an information MS [14], [15], [16], which can be integrated with antennas to form a novel architecture for wireless communication systems and establish a connection between digital signals and electromagnetic waves. However, the existence of active devices inevitably leads to the natural disadvantages of a complex structure and high cost of an active MS antenna, which can interfere with the electromagnetic field distribution of the MS antenna and thus affect its performance.

On the other hand, the passive MS antenna changes the electromagnetic field distribution by regulating the relative position between the MS and the antenna, so as to realize a change in antenna operating frequency [17], polarization characteristics [18], and directional pattern performance [19]. The polarization reconfiguration aspect that this paper focuses on has seen the implementation of some clever designs that play a crucial role in engineering. For instance, in reference [20], the relative position of the MS and the antenna was mechanically adjusted to enhance both the

The associate editor coordinating the review of this manuscript and approving it for publication was Wanchen Yang.

antenna bandwidth and gain while ensuring the preservation of the polarization characteristics. Another solution is to employ a multilayer MS design, with each layer having its designated role. This approach allows the antenna to not only achieve other performance enhancements, but also acquire polarization-reconfigurable characteristics [21]. Unfortunately, the aforementioned MS reconfigurable antennas in the above research only achieve conversion between single-line polarization and single-circular polarization characteristics, without considering dual-polarized MS reconfigurable antennas that can enhance channel capacity. Therefore, it is necessary to design a reconfigurable antenna with dual polarization that can simultaneously transform orthogonal dual-polarization characteristics.

In this paper, we propose a design method for a reconfigurable MS antenna suitable for converting between orthogonal dual linear polarization and orthogonal dual circular polarization using characteristic mode analysis, and complete the design of the 3.5GHz antenna with a center frequency. The antenna is composed of four layers: the MS, radiation patch, feed layer, and reflector plate. In addition to its superior performance, the antenna can also adjust the relative position between the MS and radiating patch layer by rotating the MS to flexibly achieve mutual transformation between orthogonal dual-linear polarization (Horizontal polarization/ Vertical polarization) and orthogonal dual-circular polarization (Left-handed circular polarization (LHCP)/right-handed circular polarization (RHCP)).

II. ANTENNA DESIGN METHODOLOGY

This paper proposes a design method for a dual-polarization reconfigurable microstrip antenna loaded with an MS to meet the design requirements of a dual-polarization reconfigurable antenna. The overall design process of the antenna is illustrated in FIGURE 1. First, the selected MS structure was analyzed using the equivalent circuit method to assess the feasibility of converting between linear and circular polarizations. Second, after conducting a characteristic mode analysis on the MS, the structure and position of the orthogonal dual-feeder are designed based on the obtained results from the surface current distribution. Finally, a superior structure was determined using full-wave simulation software to achieve balanced optimization of the performance parameters of the proposed microstrip antenna.

A. FEASIBILITY ANALYSIS OF POLARIZATION RECONSTRUCTION TO METASURFACE BY EQUIVALENT CIRCUIT METHOD

From the perspective of an equivalent circuit, if the MS is excited in a specific direction and exhibits structural symmetry in two orthogonal components of the excitation direction, two equivalent impedances with identical amplitudes and phases can be generated. Consequently, two electric field components with the same amplitude and phase can be excited in the two orthogonal directions, resulting in the synthesis of a linearly polarized wave. In contrast, if the MS

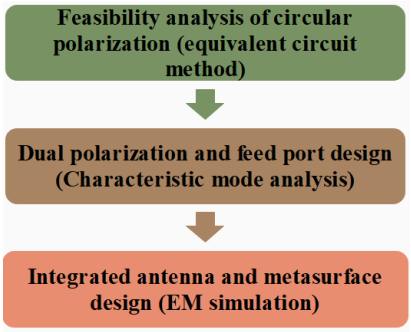

FIGURE 1. The design process of dual-polarization reconfigurable MS antenna.

exhibits structural asymmetry in its two orthogonal components of the excitation direction, it is possible to generate two equivalent impedances with identical amplitudes and a phase difference of 90°. Then, as long as the structural parameters are properly adjusted, two electric field components with the same amplitude and a phase difference of 90° are excited accordingly, resulting in the synthesis of the circularly polarized wave. According to the generation mechanism of linear and circular polarizations, if the designed MS can achieve structural symmetry and asymmetric transformation in the two orthogonal components of the excitation direction, it is feasible to realize conversion between linear and circular polarizations. An MS composed of equilateral tangential square elements can easily meet the above requirements, as shown in FIGURE 2(a). Considering the excitation along the **E** direction, the equivalent impedances along the orthogonal components $\mathbf{E}_1$ and $\mathbf{E}_2$ are equal because the MS structure is symmetric in both directions, which can be expressed as:

$$\mathbf{Z}_1 = \mathbf{Z}_2 = 2\mathrm{R} + \mathrm{j}\omega(2\,\mathrm{L}) + \frac{1}{\mathrm{j}\omega\mathrm{C}} = |\mathbf{Z}_1|\angle\varphi = |\mathbf{Z}_2|\angle\varphi \tag{1}$$

where R and L are the equivalent resistance and inductance of the MS element along $\mathbf{E}_1$ and $\mathbf{E}_2$, respectively, C is the equivalent capacitance between the gaps of the two elements along $\mathbf{E}_1$ and$\mathbf{E}_2$. Thus, two electric field components with the same amplitude and phase can be obtained in the directions of $\mathbf{E}_1$ and $\mathbf{E}_2$, respectively, allowing for the synthesis of linearly polarized waves.

The structure of the metasurface is shown in FIGURE 2(b) when the excitation direction is changed to **E**', while the equivalent impedances along the orthogonal components of $\mathbf{E}_1$' and $\mathbf{E}_2$' directions are as follows:

$$\mathbf{Z}_1' = 2\mathrm{R}_1 + \mathrm{j}\omega\,(2\mathrm{L}_1) + \frac{1}{\mathrm{j}\omega\mathrm{C}_1} = \left|\mathbf{Z}_1'\right|\angle\varphi_1 \tag{2}$$

$$\mathbf{Z}_2' = 2\mathrm{R}_2 + \mathrm{j}\omega\,(2\mathrm{L}_2) + \frac{1}{\mathrm{j}\omega\mathrm{C}_2} = \left|\mathbf{Z}_2'\right|\angle\varphi_2 \tag{3}$$

Because of the asymmetry of the MS structure in the $\mathbf{E}_1$'and $\mathbf{E}_2$' directions, circularly polarized waves can be synthesized by adjusting the metasurface structure parameters such that $\mathbf{Z}_1^{'}$and $\mathbf{Z}_2^{'}$ satisfy $\left|\mathbf{Z}_1'\right| = \left|\mathbf{Z}_2'\right|$ and $\varphi_1 - \varphi_2 = \pm 90°$.

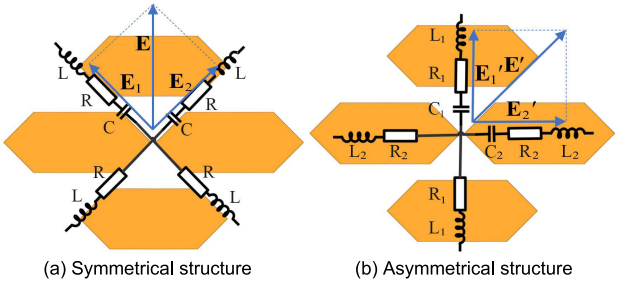

FIGURE 2. Equivalent circuit of MS.

The above analysis shows that the MS, which is composed of equilateral tangential square elements, is roughly evaluated using the equivalent circuit method. The feasibility of the MS structure to achieve polarization characteristic conversion is preliminarily verified, which lays the foundation for introducing characteristic mode analysis to guide the design of MS antennas.

B. DUAL POLARIZATION AND FEED NETWORK DESIGN BASED ON CHARACTERISTIC MODE ANALYSIS

After determining the general appearance of the MS, we conducted a preliminary design for the 3.5GHz frequency and further optimized it using CST software. The designed structure of the MS is illustrated in FIGURE 3. Subsequently, the results of the characteristic mode analysis were utilized to guide the design of both the dual-polarization feed position and the reconfigurable realization method for the MS antenna.

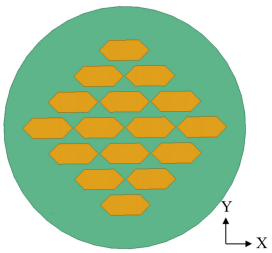

FIGURE 3. Structure of the metasurface.

In this paper, the characteristic modal analysis of the designed MS was performed using CST software. FIGURE 4 and 5 show the characteristic mode values and characteristic angles of the selected modes near 3.5GHz.As shown in FIGURE 4, modes numbered 1-6 can be excited around the observation of frequencies near 3.5GHz due to their characteristic mode values approximate or exceed 0.707. The difference between the characteristic angles of modes 1 and 2, as shown in FIGURE 5(a), was 0°, while the difference between the characteristic angles of modes 1 and 3 was 180°. These differences satisfy the conditions for generating horizontally or vertically (X/Y direction) linearly polarized waves. The mode current distributions of the designed MS modes 1 and 2 are shown in FIGURE 6(a). Conversely, according to the principle of vector orthogonality, if the MS is excited in the synthetic direction X1 shown in FIGURE 6(a), the response current components of modes 1 and 3 shown in FIGURE 6(a) can be obtained simultaneously, thus generating horizontally (X-direction) polarized waves. Similarly, as shown in FIGURE 6(b), if the MS is excited in the X2 direction, both Mode 1 and Mode 3 response current components can be obtained, resulting in vertically (Y direction) linearly polarized waves in the Y direction. Considering the case of circular polarization, as shown in FIGURE 5(b), the difference between the characteristic angles of modes 4 and 5 is 90°, and the difference between the characteristic angles of modes 6 and 5 is −90°, which satisfies the conditions for generating left-handed/right-handed circularly polarized waves. Similar to the linear polarization mechanism mentioned above, as shown in FIGURE 6(c) and 6(d), when the MS is excited in the direction of X3 or X4, it can generate left-handed/right-handed circularly polarized waves, respectively.

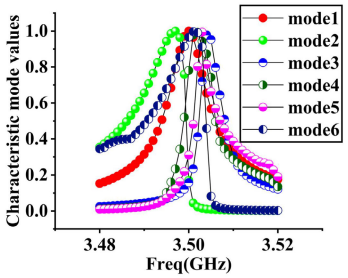

FIGURE 4. Characteristic mode values.

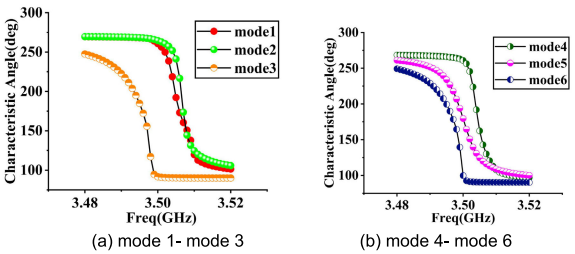

FIGURE 5. Characteristic angle.

Combined with the above analysis, as shown in FIGURE 6(a) and 6(b), X1 and X2 are mutually orthogonal. If the MS is excited simultaneously in these two directions, dual linearly polarized waves can be generated. Similarly, X3 and X4 were orthogonal to each other. If the MS is simultaneously excited in these two directions, it can produce left-handed/right-handed circularly polarized waves. Additionally, X1 and X2 can be rotated 45 ° counterclockwise to obtain X3 and X4, respectively, and vice versa. In other words, by changing the excitation direction of the MS, it is possible to achieve mutual conversion between

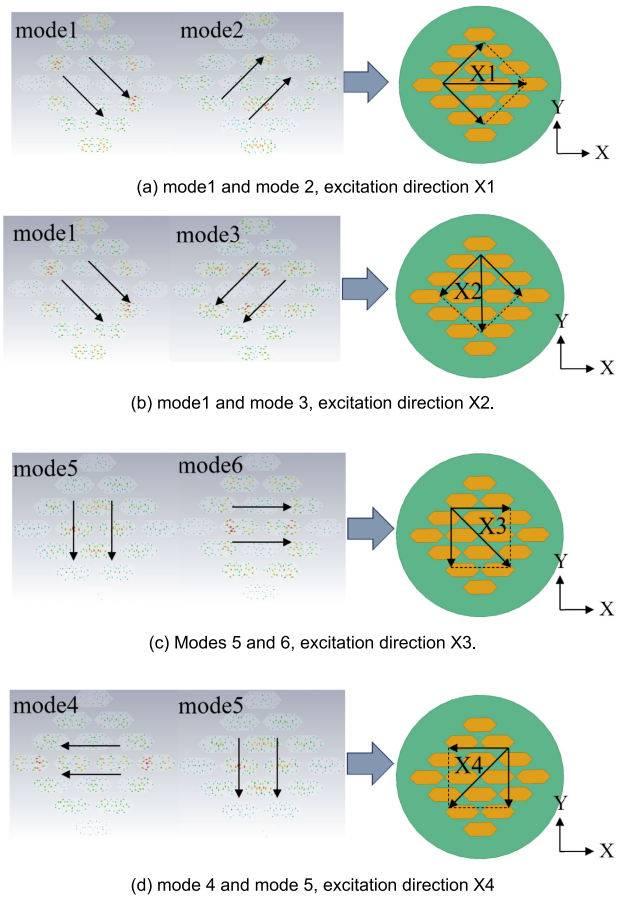

FIGURE 6. Mode current distribution and vector synthesis.

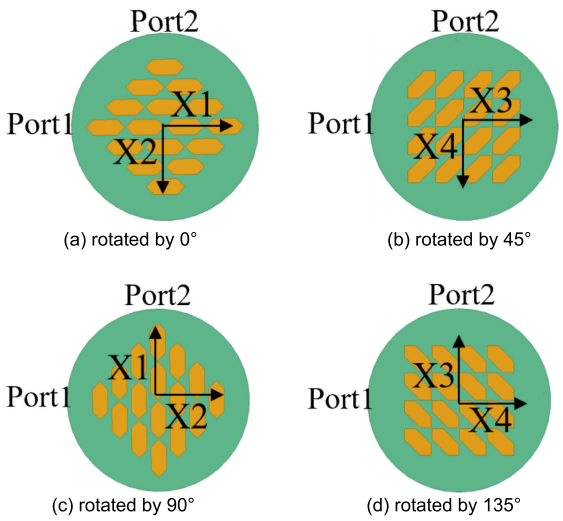

FIGURE 7. The morphology of MS under different rotation angles.

TABLE 1. Polarization characteristics of the metasurface in each morphology.

Figure	FIGURE 7. (a)	FIGURE 7. (b)	FIGURE 7. (c)	FIGURE 7. (d)
Rotating Angle	0°	45°	90°	135°
Port 1	X-linear polarization	Left-handed circular polarization	Y-linear polarization	Right-handed circular polarization
Port 2	Y-linear polarization	Right-handed circular polarization	X-linear polarization	Left-handed circular polarization

dual-linearly polarized waves and dual-circularly polarized waves. Inspired by this mechanism, in practice, the MS antenna is designed as a multilayer structure, and the excitation directions of ports 1 and 2 are fixed in the feed layer beneath the MS. By rotating the relative positions of the MS and the feed layer, the dual-linear polarization excitation direction X1/X2 is converted to the dual-circular polarization excitation direction X3/X4. Thus, the design goal of mutual transformation between dual-linear polarization and dual-circular polarization of the antenna was achieved. The morphology of the MS during counterclockwise rotation at 0°, 45°, 90°, and 135° is illustrated in FIGURE 7. The polarization characteristics of the designed MS for each morphology are listed in TABLE 1.

C. ANTENNA AND METASURFACE INTEGRATED DESIGN

According to the dual-polarization feeding mode and polarization-reconfigurable implementation scheme mentioned above, combined with advanced methods to improve the performance of the MS antenna, the MS antenna is designed in four layers: MS layer, radiation patch layer, feed layer, and reflector layer from top to bottom. The shape of each layer is designed as a circle with a radius of 126.5 mm in order to facilitate the rotation of the MS. The assembly schematic of the antenna is shown in FIGURE 8(a), and its cross section is shown in FIGURE 8(b). The medium plate selected for the MS, patch, and feed layers was Rogers 4350 (Relative permittivity = 3.66, Relative permeability = 1) with a thickness of 0.508 mm, while the reflector was made of a copper plate. The MS layer consisted of 16 square tangential copper elements, as shown in FIGURE 8.(c), with Wc = 37mm, a = 22mm, Sc = 1mm. The radiation layer is constructed with a square metal patch measuring W2 = 29.9 mm and L2 = 29.9 mm, as shown in Figure 8(d). According to the Fabry-Perot resonator theory [22], the height between the layers of the antenna is roughly specified to enhance the overall antenna gain. The feed layer consisted of two Cu-coated surfaces. The upper surface is equipped with two orthogonally placed H-shaped gaps to expand the impedance bandwidth, while the lower surface comprises two vertically positioned 50 Ω feed microstrip lines, meeting the design requirements for the dual-polarization feeding mode. The structure is shown in FIGURE 8.(e). Finally, based on the previous design, the full-wave simulation software HFSS was used to optimize the overall MS antenna. The optimized antenna structural parameters were obtained by considering the balance between various performance indicators, as shown in TABLE 2.

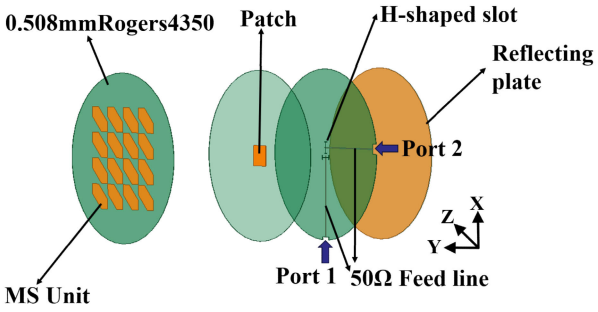

(a) Schematic assembly of antenna

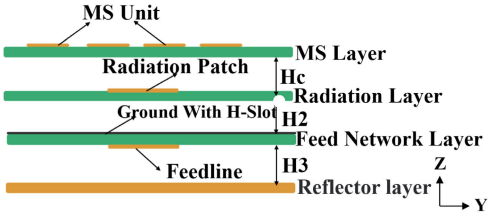

(b) Cross section drawn.

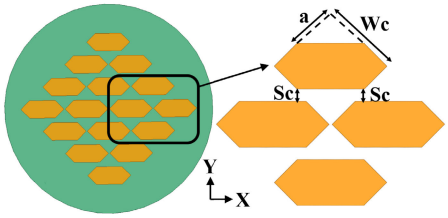

(c) Specific structure of MS

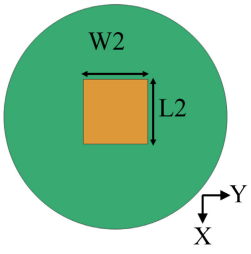

(d) Specific structure of the radiating patch

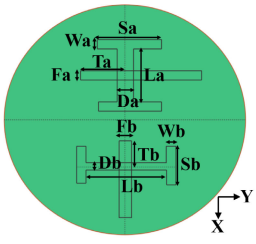

(e) Cross-placed H-shaped gaps.

FIGURE 8. The structure of the designed MS antenna.

III. SIMULATION AND MEASUREMENT RESULTS

To verify the effectiveness of the designed antenna, the HFSS full-wave solver was used to simulate the S-parameter, direction pattern, axis ratio, and other performance parameters of the antenna, and compared with the measured results of the antenna. The designed antenna and the actual measurement environment are shown in FIGURE 9.

TABLE 2. The structural parameters of the designed antenna.

MS and Patch Layer	**a**	**Sc**	**Wc**	**W2**	**L2**
	22mm /0.26λ_0	1mm /0.01λ_0	37mm /0.43λ_0	29.9mm /0.35λ_0	29.9mm /0.35λ_0
Feed Network Layer	**Sa**	**Wa**	**Ta**	**Fa**	**La**
	4.9mm /0.06λ_0	0.95mm /0.01λ_0	4.75mm /0.05λ_0	1.04mm /0.01λ_0	12mm /0.14λ_0
	Da	**Fb**	**Wb**	**Tb**	**Db**
	0.5mm /0.01λ_0	22mm /0.26λ_0	0.95mm /0.01λ_0	4.4mm /0.05λ_0	0.5mm /0.01λ_0
	Sb	**Lb**			
	5.4mm /0.05λ_0	11.65mm /0.14λ_0			
Interlayer Spacing	**Hc**	**H2**	**H3**		
	44mm /0.51λ_0	8mm /0.1λ_0	8mm /0.1λ_0		

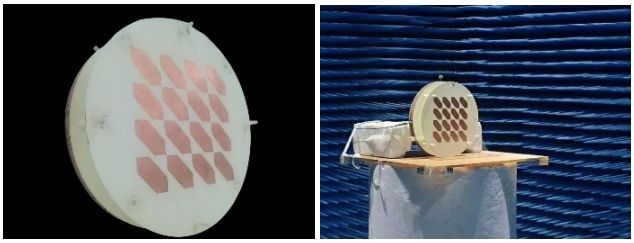

(a) Design antenna (b) Antenna measurement environment

FIGURE 9. Antenna and measurement.

A. S PARAMETER

The S-parameters of the designed antenna under the four morphologies with MS rotation angles of 0°, 45°, 90°, and 135° are shown in FIGURE 10. It can be observed that the simulation results agree well with the measured results. Owing to the symmetry of the MS antenna structure, the results are shown in FIGURE 10.(a), and FIGURE 10.(c) were similar. The −10 dB impedance bandwidths of S11 and S22 are approximately 11.4%, and S21 is less than −40 dB at the center frequency of 3.5GHz. For the same mechanism, the results are shown in FIGURE 10.(b), and FIGURE 10.(d) are similar. The −10 dB impedance bandwidths of S11 and S22 are approximately 11.4%, and S21 is less than -20 dB at a center frequency of 3.5 GHz. This shows that, in the designed frequency band, when the MS rotates in different positions, the two ports are well matched, and the ports have high isolation.

B. RADIATION PATTERN

Considering the reciprocity between the two feed structures of the designed antenna, including the feed microstrip line and H-slot, and the symmetry of the MS structure, the antenna fed by port 2 can be equivalent to the antenna fed by port 1 after the MS is rotated by 90° when analyzing the antenna

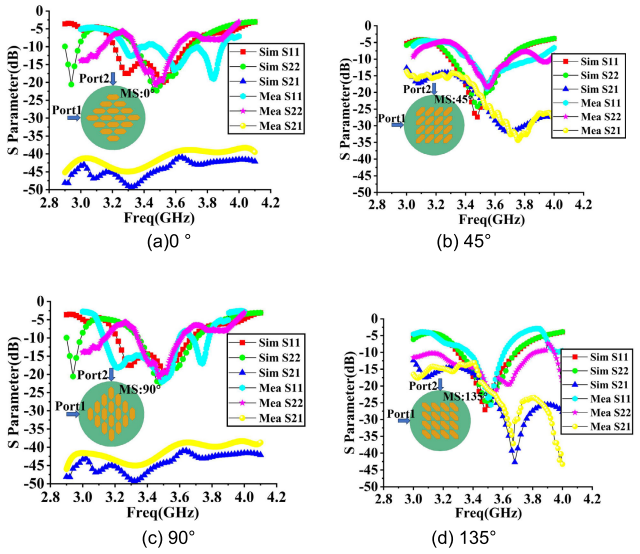

FIGURE 10. Simulated and measured S parameter for MS under different rotation angle.

pattern characteristics. For example, the port 2 feed state of the MS with a 0° attitude is equivalent to the port 1 feed state of the MS with a 90° attitude. Similarly, the feed equivalence of ports 1 and 2 under each MS rotation attitude is presented in TABLE 3.

By analyzing the radiation pattern of the MS antenna fed by port 1 under the four rotating attitudes of the MS, the radiation characteristics of the MS antenna fed by port 2 can be equivalently obtained. Based on the orthogonality of the port position, the analysis of radiation characteristics from only one port is sufficient for dual-polarized antennas because the two ports work simultaneously and do not interfere with each other. The measured and simulated radiation patterns from the E-plane and H-plane of the antenna with 3.5 GHz excited by port 1 for different MS attitudes are shown in FIGURE 11. It can be seen from this result that under the attitude of MS 0° and MS 90°, the main polarization mode of the antenna is linear polarization in the X and Y directions, respectively. The antenna gain is 13 dBi, and the cross-polarization isolation degree is greater than 40 dB. For MS angles of 45° and 135°, the main polarization modes of the antenna at are left-handed circular polarization and right-handed circular polarization, respectively. The gain of the antenna is 13 dBi, and the cross-polarization isolation degree is greater than 20 dB. These measured results are in accordance with the design results of the antenna, especially the high cross isolation, which guarantees the dual polarization of the antenna.

C. AXIAL RATIO (AR)

According to the analysis in the previous section, when analyzing the Axis Ratio (AR) of the designed antenna, this paper also adopts a scheme that only analyzes the response of the port 1 feed and performs an equivalent calculation of the port 2 feed. FIGURE 12 shows the simulation and

TABLE 3. The equivalence of port 1 and port 2 for each metasurface rotation attitude.

MS rotation attitude	0°	45°	90°	135°
Port 1	90°/Port2	135°/Port2	0°/Port2	45°/Port2
Port 2	90°/Port1	135°/Port1	0°/Port1	45°/Port1

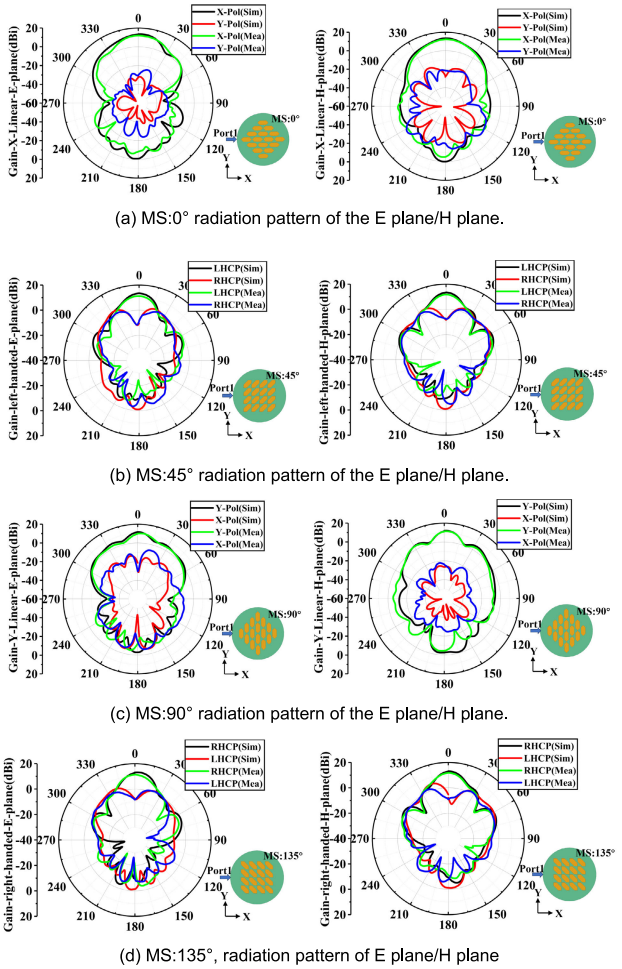

FIGURE 11. Simulated and measured radiation patterns at 3.5 GHz.

measurement results of the antenna axial ratio under circular polarization (left-handed circular polarization/MS 45° and Right-handed circular polarization /MS135°). It can be seen that the axial ratio of the antenna AR is less than 3 dB in the band range of 3.3 GHz to 3.8 GHz under circular polarization, and the axial specific bandwidth is about 500 MHz.

TABLE 4 presents a performance comparison among several polarization-reconfigurable antennas that achieve polarization switching by rotating the MS. The main contribution of the proposed antenna is its ability to flexibly convert between double linear polarization and double circular polarization while maintaining good polarization cross-isolation, which distinguishes it from other similar antennas [23], [24],

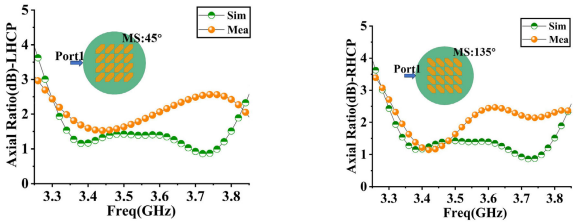

(a) MS:45° (b) MS:135°

FIGURE 12. Simulated and measured AR at 3.5 GHz.

TABLE 4. Performance comparison of several polarization-reconfigurable antennas.

Ref.	[23]	[24]	[25]	[26]	This Paper
Frequency (GHz)	9.5	3.5	4.35	2.4	3.5
Polarization operation	single	single	single	single	dual
3dB-AR BW(%)	33.0	11.4	2.7	17.4	17.4
Polarization isolation degree (dB)		CP:15.0 LP:50.0		CP:21.5 LP:27.2	CP:21.8 LP:42.0
Gain (dBi)	16.5	CP:5.0 LP:7.5	6.5	CP:7.2 LP:7.0	LP:13.0 CP:13.0
Electrical Size (Radius* Height)	$2.9\lambda_0$* $1.1\lambda_0$	$0.88\lambda_0$* $0.06\lambda_0$	$0.13\lambda_0$* $0.012\lambda_0$	$0.6\lambda_0$* $0.14\lambda_0$	$1.4\lambda_0$* $0.7\lambda_0$

[25], [26]. TABLE 4 presents a comparison of the electrical sizes of each antenna. Although the proposed antenna is not dominant in terms of electrical size, it achieves a balance between electrical size and performance. Compared with the reference [23], the proposed antenna has a smaller electrical size than the contrast antenna, but it also suffers from a resulting reduction in gain. Compared with references [24], [25], [26], despite the proposed antenna having a larger electrical size, it offers higher gain benefits.

IV. CONCLUSION

A dual-polarization reconfigurable antenna with a center frequency of 3.5 GHz was designed according to the design method proposed in this paper. By rotating the MS, a mutual transformation between dual-linear polarization and dual-circular polarization can be achieved. The simulation and measurement results of the antenna indicate that the antenna has a gain of 13 dBi and polarization cross isolation of 42 dB in the dual-linear polarization state. In the dual circular polarization state, the antenna maintains a gain of 13 dBi, a polarization cross isolation of 21.8 dB, and an axial ratio bandwidth with a 3dB range that can reach 17.4%.

REFERENCES

[1] J. Chocarro, J. Manuel Pérez-Escudero, J. Teniente, J. C. Iriarte-Galarregui, and I. Ederra, "A metasurface-enhanced substrate-integrated waveguide antenna," *IEEE Access*, vol. 12, pp. 62448–62458, 2024.

[2] M. Li, R. Wang, H. Yao, and B. Wang, "A low-profile wideband CP end-fire magnetoelectric antenna using dual-mode resonances," *IEEE Trans. Antennas Propag.*, vol. 67, no. 7, pp. 4445–4452, Jul. 2019.

[3] Z. Wang, S. Zhao, and Y. Dong, "Pattern reconfigurable, low-profile, vertically polarized, ZOR-metasurface antenna for 5G application," *IEEE Trans. Antennas Propag.*, vol. 70, no. 8, pp. 6581–6591, Aug. 2022.

[4] M. Li, Q. L. Li, B. Wang, C. F. Zhou, and S. W. Cheung, "A low-profile dual-polarized dipole antenna using wideband AMC reflector," *IEEE Trans. Antennas Propag.*, vol. 66, no. 5, pp. 2610–2615, May 2018.

[5] Y. Hao, C. Deng, X. Cao, Y. Yin, and K. Sarabandi, "A high aperture efficiency 1-bit reconfigurable reflectarray antenna with extremely low power consumption," *IEEE Trans. Antennas Propag.*, vol. 72, no. 1, pp. 1015–1020, Jan. 2024.

[6] H. Rajabalipanah, A. Abdolali, J. Shabanpour, A. Momeni, and A. Cheldavi, "Asymmetric spatial power dividers using phase-amplitude metasurfaces driven by Huygens principle," *ACS Omega*, vol. 4, no. 10, pp. 14340–14352, 2019.

[7] K. M. Kossifos, J. Georgiou, and M. A. Antoniades, "ASIC-enabled programmable metasurfaces—Part 1: Design and characterization," *IEEE Trans. Antennas Propag.*, vol. 72, no. 3, pp. 2790–2799, Mar. 2024.

[8] K. Chen, N. Zhang, G. Ding, J. Zhao, T. Jiang, and Y. Feng, "Active anisotropic coding metasurface with independent real-time reconfigurability for dual polarized waves," *Adv. Mater. Technol.*, vol. 5, no. 2, Feb. 2020, Art. no. 1900930.

[9] Z. Wu, H. Liu, and L. Li, "Metasurface-inspired low profile polarization reconfigurable antenna with simple DC controlling circuit," *IEEE Access*, vol. 7, pp. 45073–45079, 2019.

[10] Z. Wang and Y. Dong, "Amplitude and frequency modulated leaky wave antenna for reconfigurable intelligent radiation," *IEEE Trans. Antennas Propag.*, vol. 72, no. 3, pp. 2189–2201, Mar. 2024.

[11] M. A. Sufian, N. Hussain, H. Askari, S. G. Park, K. S. Shin, and N. Kim, "Isolation enhancement of a metasurface-based MIMO antenna using slots and shorting pins," *IEEE Access*, vol. 9, pp. 73533–73543, 2021.

[12] S. Li, F. Xu, X. Wan, T. J. Cui, and Y.-Q. Jin, "Programmable metasurface based on substrate-integrated waveguide for compact dynamic-pattern antenna," *IEEE Trans. Antennas Propag.*, vol. 69, no. 5, pp. 2958–2962, May 2021.

[13] Z. Wang, X. Pan, F. Yang, S. Xu, M. Li, and D. Su, "Design, analysis, and experiment on high-performance orbital angular momentum beam based on 1-Bit programmable metasurface," *IEEE Access*, vol. 9, pp. 18585–18596, 2021.

[14] T. J. Cui, S. Liu, and L. Zhang, "Information metamaterials and metasurfaces," *J. Mater. Chem. C*, vol. 5, no. 15, pp. 3644–3668, 2017.

[15] S. Liu and T. J. Cui, "Flexible controls of terahertz waves using coding and programmable metasurfaces," *IEEE J. Sel. Topics Quantum Electron.*, vol. 23, no. 4, pp. 1–12, Jul. 2017.

[16] L. Zhang, X. Q. Chen, S. Liu, Q. Zhang, J. Zhao, and J. Y. Dai, "Space time coding digital metasurfaces," *Nature Commun.*, vol. 9, no. 1, p. 4334, 2018.

[17] H. L. Zhu, X. H. Liu, S. W. Cheung, and T. I. Yuk, "Frequency-reconfigurable antenna using metasurface," *IEEE Trans. Antennas Propag.*, vol. 62, no. 1, pp. 80–85, Jan. 2014.

[18] H. L. Zhu, S. W. Cheung, K. L. Chung, and T. I. Yuk, "Linear-to-circular polarization conversion using metasurface," *IEEE Trans. Antennas Propag.*, vol. 61, no. 9, pp. 4615–4623, Sep. 2013.

[19] N. Nguyen-Trong, L. Hall, and C. Fumeaux, "A frequency-and pattern-reconfigurable center-shorted microstrip antenna," *IEEE Antennas Wireless Propag. Lett.*, vol. 15, pp. 1955–1958, 2016.

[20] H. L. Zhu, S. W. Cheung, and T. I. Yuk, "Mechanically pattern reconfigurable antenna using metasurface," *IET Microw., Antennas Propag.*, vol. 9, no. 12, pp. 1331–1336, Sep. 2015.

[21] B. Majumder, K. Krishnamoorthy, J. Mukherjee, and K. P. Ray, "Frequency-reconfigurable slot antenna enabled by thin anisotropic double layer metasurfaces," *IEEE Trans. Antennas Propag.*, vol. 64, no. 4, pp. 1218–1225, Apr. 2016.

[22] H. H. Tran and H. C. Park, "A simple design of polarization reconfigurable Fabry–Pérot resonator antenna," *IEEE Access*, vol. 8, pp. 91837–91842, 2020.

[23] C. Ni, M. S. Chen, Z. X. Zhang, and X. L. Wu, "Design of frequency-and polarization-reconfigurable antenna based on the polarization conversion metasurface," *IEEE Antennas Wireless Propag. Lett.*, vol. 17, pp. 78–81, 2018.

[24] H. L. Zhu, S. W. Cheung, X. H. Liu, and T. I. Yuk, "Design of polarization reconfigurable antenna using metasurface," *IEEE Trans. Antennas Propag.*, vol. 62, no. 6, pp. 2891–2898, Jun. 2014.
[25] K. Kandasamy, B. Majumder, J. Mukherjee, and K. P. Ray, "Low-RCS and polarization-reconfigurable antenna using cross-slot-based metasurface," *IEEE Antennas Wireless Propag. Lett.*, vol. 14, pp. 1638–1641, 2015.
[26] Y. Wan, H. Chen, Q. Chen, and W.-M. Zou, "A polarization-reconfigurable antenna with tunable axial-ratio bandwidth using metasurface," in *Proc. IEEE Asia–Pacific Microw. Conf. (APMC)*, Dec. 2019, pp. 1185–1187.

BO WU received the Ph.D. degree in physical electronics from Anhui University of China, Hefei, in 2013. He is currently an Associate Professor with the School of Electronics and Information Engineering, Anhui University. His current research interests include computational electromagnetic and antenna design.

PENGDONG JI is currently a Graduate Student jointly trained by the School of Electronics and Information Engineering, Anhui University, and Anhui Province Key Laboratory of Simulation and Design for Electronic Information System, Hefei Normal University. His current research interest includes integrated design of metasurface antennas.

YANG LI is currently pursuing the bachelor's degree with Anhui Province Key Laboratory of Simulation and Design for Electronic Information System, Hefei Normal University. His research interests include microwave devices and antenna design.

ZHENWEI LIU is currently pursuing the bachelor's degree with Anhui Province Key Laboratory of Simulation and Design for Electronic Information Systems, Hefei Normal University. His research interests include microwave devices and antenna design.

LIANG ZHANG received the Ph.D. degree in electromagnetic field and microwave technique from Anhui University of China, Hefei, in 2010. He is currently a Professor with Anhui Province Key Laboratory of Simulation and Design for Electronic Information System, Hefei Normal University. His current research interests include fast measurement method of antenna near and far field and compressive sensing.

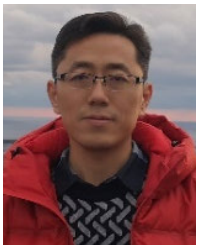

ZHONGXIANG ZHANG received the Ph.D. degree in electromagnetic field and microwave technique from the University of Science and Technology of China, Hefei, in 2007. He is currently a Professor with Anhui Province Key Laboratory of Simulation and Design for Electronic Information System, Hefei Normal University. His current research interests include electromagnetic field and microwave technology, millimeter wave radar, and 5G mobile communication base station antenna.

MENG KONG received the M.S. and Ph.D. degrees in electromagnetic field and microwave technique from Anhui University of China, Hefei, in 2009 and 2016, respectively. He is currently a Professor with Anhui Province Key Laboratory of Simulation and Design for Electronic Information System, Hefei Normal University. His current research interests include computational electromagnetic and antenna design.